



Title	Calcium phosphate coating on dental composite resins by a laser-assisted biomimetic process
Author(s)	Nathanael, A. Joseph; Oyane, Ayako; Nakamura, Maki; Koga, Kenji; Nishida, Erika; Tanaka, Saori; Miyaji, Hirofumi
Citation	Heliyon, 4(8), UNSP e00734 <a href="https://doi.org/10.1016/j.heliyon.2018.e00734">https://doi.org/10.1016/j.heliyon.2018.e00734</a>
Issue Date	2018-08
Doc URL	<a href="http://hdl.handle.net/2115/71746">http://hdl.handle.net/2115/71746</a>
Rights(URL)	<a href="http://creativecommons.org/licenses/by-nc-nd/4.0/">http://creativecommons.org/licenses/by-nc-nd/4.0/</a>
Type	article
File Information	miyaji_1-s2.0-S2405844018310430-main.pdf



[Instructions for use](#)

Received:  
14 March 2018  
Revised:  
15 June 2018  
Accepted:  
8 August 2018

Cite as: A. Joseph Nathanael, Ayako Oyane, Maki Nakamura, Kenji Koga, Erika Nishida, Saori Tanaka, Hirofumi Miyaji. Calcium phosphate coating on dental composite resins by a laser-assisted biomimetic process. *Heliyon* 4 (2018) e00734. doi: [10.1016/j.heliyon.2018.e00734](https://doi.org/10.1016/j.heliyon.2018.e00734)



# Calcium phosphate coating on dental composite resins by a laser-assisted biomimetic process

A. Joseph Nathanael<sup>a</sup>, Ayako Oyane<sup>a,\*</sup>, Maki Nakamura<sup>a</sup>, Kenji Koga<sup>a</sup>, Erika Nishida<sup>b</sup>, Saori Tanaka<sup>b,c</sup>, Hirofumi Miyaji<sup>b</sup>

<sup>a</sup> *Nanomaterials Research Institute, National Institute of Advanced Industrial Science and Technology (AIST), Central 5, 1-1-1 Higashi Tsukuba, 305-8565, Japan*

<sup>b</sup> *Department of Periodontology and Endodontology, Faculty of Dental Medicine, Hokkaido University, N13W7, Kita-ku, Sapporo 060-8586, Japan*

<sup>c</sup> *Division of General Dentistry Center for Dental Clinics, Hokkaido University Hospital, N14W5, Kita-ku, Sapporo 060-8648, Japan*

\* Corresponding author.

E-mail address: [a-oyane@aist.go.jp](mailto:a-oyane@aist.go.jp) (A. Oyane).

## Abstract

**Objectives:** Dental composite resins with better biocompatibility and osteoconductivity have been sought in endodontic treatments. This study aimed to develop a technique to produce the osteoconductive resin surfaces through calcium phosphate (CaP) coating using a laser-assisted biomimetic (LAB) process.

**Methods:** Light-cured, acrylic-based composite resins were used as substrates. The resin substrate was subjected to a LAB process comprising Nd:YAG pulsed laser irradiation in a supersaturated CaP solution. The LAB-processed substrate was immersed for 3 days in a simulated body fluid (SBF) for the preliminary osteoconductivity assessment.

**Results:** After irradiation for 30 min, the resin surfaces were partly coated with a newly formed CaP layer. The coating layer contained hydroxyapatite as the main crystalline phase and the coating coverage depended on the laser wavelength and

the type of resin. The LAB-processed CaP-coated surface exhibited apatite-forming ability in SBF.

**Conclusions:** LAB process is effective for CaP coating on light-cured dental composite resins and improving their osteoconductivity.

**Clinical significance:** The LAB process is a potential new tool to create a cementum-like osteoconductive surface on dental composite resins.

Keywords: Biomedical engineering, Dentistry, Materials science

## 1. Introduction

Dental composite resins composed of an organic polymer matrix and inorganic ceramic fillers have been used as restorative and/or adhesive materials in dentistry. Dental composite resins are usually prepared during the treatment by curing mixed raw materials, that is, inorganic ceramic fillers, acrylate- or epoxy-based monomers, and additives, *via in situ* polymerization. In the past few decades, these resins have evolved significantly, with maximum development concentrating on the filler technology for easier handling and production of materials with better mechanical properties, tooth-like appearance, higher wear resistance, minimal shrinkage, and release capability for therapeutic components [1, 2, 3]. However, dental composite resins can still be improved with regard to their surface biocompatibility and osteoconductivity. For example, when the dental composite resins are used as root repair materials for root-end sealing or to repair root perforations or external root resorptions, the exposed resin surfaces rarely allow for the reconstruction of periodontal attachments due to their nonosteoconductive nature. In the periodontal attachments in healthy natural teeth, the cementum tissue, which is composed of calcium phosphate (CaP) compounds [mainly hydroxyapatite (HA)] and collagen, plays an important role as a connector that attaches the tooth root to the surrounding alveolar bone. However, several composite resins are liable to induce fibrous tissue formation on their surfaces rather than regenerating the cementum tissue [4], and may cause widening of the periodontal ligament space [5]. Insufficient periodontal attachment may impair occlusal support and increase the risk of infection.

Conventional filler-based approaches have limitations in improving the surface biological properties of dental composite resins because the majority of the cured resin's surface is occupied by a bioinert polymer matrix. Postcuring surface functionalization, more specifically, CaP coating over a cured dental composite resin would be an effective approach to provide the resin surface with osteoconductivity through an artificially created cementum-like surface. Some CaP compounds, such as HA,  $\beta$ -tricalcium phosphate, and octacalcium phosphate (OCP), have been reported to exhibit good biocompatibility and osteoconductivity, and have an excellent safety record as restorative and grafting materials for hard tissues [6, 7, 8].

Although there are various CaP coating techniques for biomaterials [8, 9] (typically plasma spraying [10]), a majority of them are not usable for surface functionalization of cured dental composite resins due to practical and/or safety issues. To implement on-site and postcuring CaP coating on dental composite resins, the process should be conducted under normal pressure and temperature, and should be facile enough to accomplish within a normal treatment time (a few tens of minutes or less). In addition, the coating area should be finely confined to the target region in the affected part, *i.e.*, the exposed surface of a cured dental composite resin facing the soft and hard periodontal tissues. Furthermore, the coating medium should contain no harmful components and must be intraorally administrable. Recently, the authors developed a CaP coating technique using a laser-assisted biomimetic (LAB) process that satisfies these requirements [11, 12, 13, 14, 15, 16]. In the LAB process, a weak pulsed Nd:YAG laser is used to irradiate the target region of an artificial material immersed in a supersaturated CaP solution. Within only 10–30 min, CaP, that is, HA and/or OCP, precipitates on the laser-irradiated region of the material's surface. The authors have previously demonstrated that the LAB process is effective for CaP coating on various artificial materials with laser light absorption such as organic polymers [12, 13], ceramics [14], and metals [15, 16]. The authors hypothesized that CaP coating on cured dental composite resins is feasible using our LAB process, and that the resulting CaP-coated resin surfaces would possess osteoconductivity. To verify these hypotheses, substrates of light-cured composite resins were subjected to the LAB process using a supersaturated CaP solution (denoted as CP solution [17]). The LAB-processed resin surfaces were characterized and compared to the untreated surfaces. Following the LAB process, the resin substrates were immersed in a simulated body fluid (SBF) [18], with ion concentrations approximately equal to those of human blood plasma, for preliminary assessment of the *in vivo* osteoconductivity of the LAB-processed resin surfaces.

## 2. Materials and methods

### 2.1. Preparation and optical evaluation of resin substrates

Two dental composite resins were used: Beautifil Flow Plus A3 [denoted as BA3, Fig. 1 (a)] and Beautifil Flow Plus CV [denoted as BCV, Fig. 3 (a)] purchased from Shofu Inc., Japan. These are acrylate-based composite resins with silica-based glass fillers. BA3 and BCV have different shades, and thus possess different optical properties.

Substrates for BA3 and BCV were prepared based on the manufacturer's protocols. Initially, the raw materials were mixed in a syringe, cast into a 1 mm-thick open mold (circular mold of 6 mm in diameter or square mold with a size of 35 mm × 35 mm), and pressed between two transparent polymer films to flatten both surfaces. Thereafter, blue LED light ( $\lambda = 380\text{--}430$  nm, 1 W/cm<sup>2</sup>) was

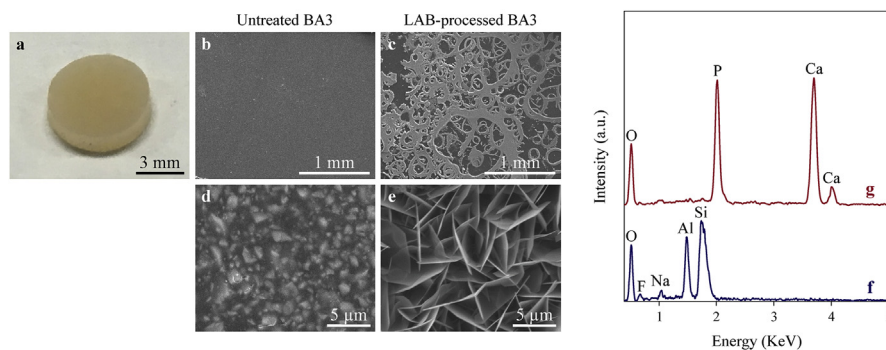


**Fig. 1.** Digital image of the BA3 substrate (a), SEM images in lower (b, c) and higher (d, e) magnifications, and EDX spectra (f, g) of the surface, before (a, b, d, f) and after (c, e, g) the LAB process. The EDX spectrum (g) was obtained from the CaP-coated region on the surface.

irradiated for 10 s using a dental curing light (PenCure, J. Morita Corporation, Japan) to cure the resin.

The cured square resin substrates (1 mm-thick, 35 mm × 35 mm in size) were used for diffuse reflection measurement using a UV–VIS–NIR spectrophotometer (SolidSpec-3700 DUV, SHIMADZU Corporation, Japan) to examine their light absorption properties. The disk-shaped resin substrates (1 mm-thick, 6 mm in diameter) were used for all other experiments described in the following sections.

## 2.2. LAB process for CaP coating

The substrate was immersed in 5 mL of the CP solution (NaCl 142 mM, CaCl<sub>2</sub> 3.75 mM, K<sub>2</sub>HPO<sub>4</sub>·3H<sub>2</sub>O 1.5 mM, HCl 40 mM, buffered to pH = 7.4 at 25 °C with 50 mM tris(hydroxymethyl)aminomethane and 1M HCl [17]), which was stored in a glass bottle and maintained at 25 °C with a temperature controlled water bath [12, 13, 14, 15, 16]. Laser irradiation was performed using the output of the second harmonic (VIS; λ = 532 nm) or third harmonic (UV; λ = 355 nm) of a Nd:YAG laser (Quanta-Ray LAB-150-30, Spectra-Physics, USA) operated at 30 Hz. The VIS laser was used in the LAB process, unless otherwise specified. The laser fluence was fixed at 4 W/cm<sup>2</sup> (133 mJ/pulse/cm<sup>2</sup>). The laser beam possessed an output diameter of 7–8 mm and was irradiated without focusing onto the substrate which was immersed in the CP solution. The irradiation conditions were determined according to our previous report on polymer substrates [13]. After irradiation for 30 min, the substrate was removed from the solution, gently washed with ultrapure water, and air-dried before further analysis.

## 2.3. Surface characterization

The surfaces of the substrates were analyzed before and after the LAB process using a field emission scanning electron microscope (SEM; S-4800, Hitachi High-

Technologies Corp., Japan) equipped with an energy-dispersive X-ray spectroscope (EDX; EMAX X-act, Horiba Scientific, Japan). Prior to the SEM and EDX analyses, the substrate surfaces were coated with carbon using a carbon coater (VC-100, Vacuum Device Inc., Japan).

Crystallographic analysis of the surface coating layers on the LAB-processed substrates was performed using a transmission electron microscope (TEM; JEM-2010, JEOL Ltd., Japan) with a LaB<sub>6</sub> filament at an acceleration voltage of 200 kV. Prior to the TEM analysis, the surface layer was gently scraped from the substrate surface and transferred onto a holey carbon grid. In the selected area electron diffraction (SAED) analysis, the camera length was set at 200 cm. In the SAED analysis, calculated diffraction profiles of hexagonal HA [HA (hex)], monoclinic HA [HA (mono)], and OCP were prepared using the pseudo-Voigt function with an instrumental resolution width determined from the sharp small spots following intensity calculation under kinematic approximation using ReciPro software ([http://pmsl.planet.sci.kobe-u.ac.jp/~seto/?page\\_id=19&lang=en](http://pmsl.planet.sci.kobe-u.ac.jp/~seto/?page_id=19&lang=en)). Calculated diffraction patterns of HA (hex), HA (mono), and OCP along the most probable zone axis for each crystalline phase were prepared using CrystalMaker and SingleCrystal software packages (CrystalMaker Software Ltd., UK).

## 2.4. SBF test for preliminary osteoconductivity assessment

The SBF test was carried out according to Kokubo's protocol [18]. Briefly, the LAB-processed substrate was immersed in 30 mL of SBF (c-SBF; NaCl 136.8 mM, NaHCO<sub>3</sub> 4.2 mM, KCl 3.0 mM, K<sub>2</sub>HPO<sub>4</sub>·3H<sub>2</sub>O 1.0 mM, MgCl<sub>2</sub>·6H<sub>2</sub>O 1.5 mM, HCl 40 mM, CaCl<sub>2</sub> 2.5 mM, Na<sub>2</sub>SO<sub>4</sub> 0.5 mM, buffered to pH = 7.40 at 36.5 °C with 50 mM tris(hydroxymethyl)aminomethane) and 1M HCl [18]). After immersion in SBF at 36.5 °C for 3 days, the substrate was gently washed with ultrapure water and air-dried. The substrate surfaces were analyzed before and after the SBF test using SEM and a thin-film X-ray diffractometer (XRD; Ultima IV, Rigaku Co., Japan).

## 3. Results and discussion

### 3.1. CaP coating on resins

Using the LAB process with the VIS laser, the BA3 resin surface was partially coated with a CaP layer. As shown in the SEM images in Fig. 1 (b, d), the untreated BA3 resin had a flat surface on a millimeter scale over which the submicro- and micro-scale fillers were sparsely and homogeneously distributed. According to its EDX spectrum [Fig. 1 (f)], the untreated BA3 resin surface contained O, F, Na, Al, and Si as the filler components. After the LAB process, more than half of the resin surface was coated with a layer [Fig. 1 (c)]. This coating layer had a plate-

like microstructure [Fig. 1 (e)], and contained O, Ca, and P as major components [Fig. 1 (g)]. This result suggests that the coating layer formed by the LAB process was composed of a CaP compound.

The LAB process for CaP coating not only was utilized for BA3 resin but also was applied to the BCV resin. The BCV resin has a different shade and thus, different optical properties from those of the BA3 resin (Fig. 2). The SEM and EDX results of the BCV resin (Fig. 3) were similar to those obtained for the BA3 resin (Fig. 1), although the coating coverage decreased for the BCV resin.

The mechanism underlying CaP formation during the LAB process can be described as follows [12]. The CP solution is a metastable supersaturated solution in which CaP spontaneously precipitates homogeneously or heterogeneously with a specific trigger. Unlike the CP solution [16], the BA3 and BCV resins absorb light at a specific level at 532 nm (Fig. 2). Therefore, the VIS laser light ( $\lambda = 532$  nm) applied to the CP solution reached the underwater resin surface with minimal attenuation and

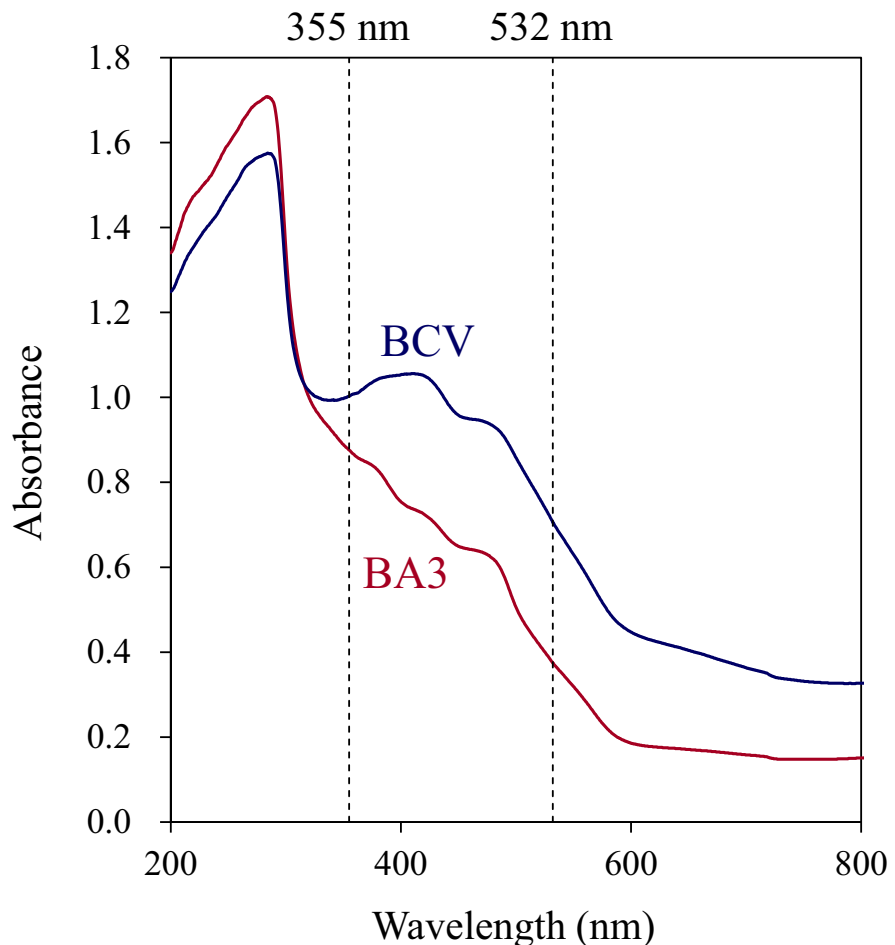
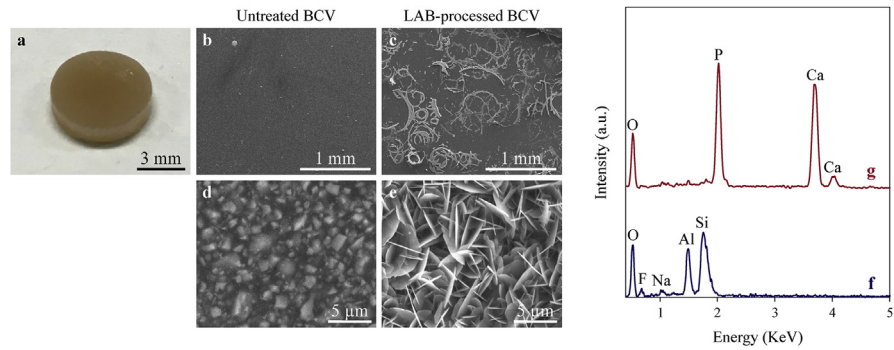


Fig. 2. Absorption spectra of the untreated BA3 and BCV substrates.



**Fig. 3.** Digital image of the BCV substrate (a), SEM images in lower (b, c) and higher (d, e) magnifications, and EDX spectra (f, g) of the surface, before (a, b, d, f) and after (c, e, g) the LAB process. The EDX spectrum (g) was obtained from the CaP-coated region on the surface.

was absorbed by the surface. The thus-absorbed laser light energy is used to heat and modify the resin surface, triggering heterogeneous CaP precipitation at the surface. Prenucleation CaP clusters [19, 20, 21] might be involved in the precipitation reactions in the CP solution.

The LAB process was performed for the BA3 resin with UV laser (at the same fluence for VIS laser) as well, since the BA3 resin revealed higher light absorption at 355 nm than at 532 nm (Fig. 2); however, the resin surface caused micrometer-scale deformation only, without the formation of CaPs (Fig. 4). This might be because the laser absorption at the tested irradiation condition was so high that the surface modification became fierce and destructive (melting, ablation, etc.), thereby undermining the stable surface required for precipitation. A similar phenomenon has been reported for titanium metal [16]. Note that the capability of CaP precipitation in the LAB process is not always proportional to the degree of laser absorption; there is an opportune level of absorption (dependent on the substrate material and irradiation conditions) for inducing moderate surface modification suitable for precipitation

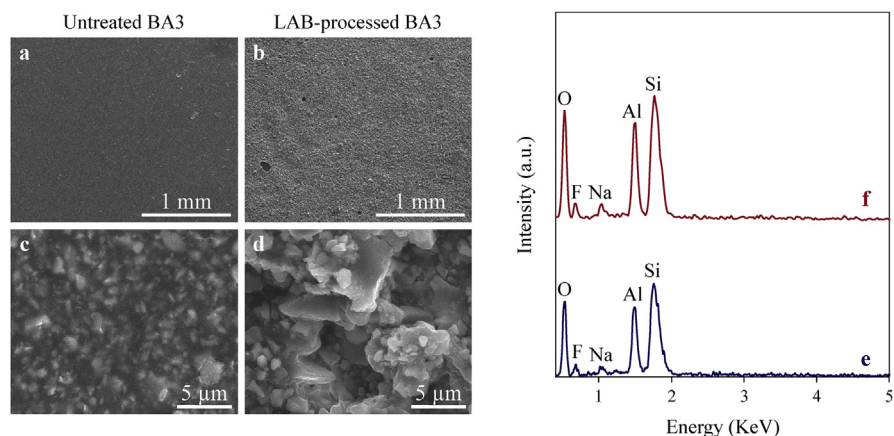


**Fig. 4.** SEM images in lower (a, b) and higher (c, d) magnifications and EDX spectra (e, f) of the surface of the BA3 substrate, before (a, c, e) and after (b, d, f) the LAB process using the UV laser.



[16]. More detailed studies are needed to fully clarify the precipitation mechanism on the resin surface and to identify the optimum irradiation condition for the LAB process to improve the coating coverage.

### 3.2. Crystallographic analysis of CaP

The CaP layer formed on the LAB-processed resin surface was most likely to be HA, although it may contain a small amount of OCP and an amorphous phase. Crystallographic analyses through TEM observations along with SAED measurements were performed for two different fragments: aggregated fragments [Fig. 5 (a)] and a plate-like single fragment [Fig. 5 (c)] sampled from the LAB-processed BA3 resin. The latter was observed to be as a piece of thin plate in the SEM image in Fig. 1 (e).

The SAED pattern from the aggregated fragments [Fig. 5 (b)] showed Debye rings indicating either polycrystalline substances or an assembly of fine particles. The rings were compared with the calculated profiles of three different CaP crystalline phases: HA (hex), HA (mono), and OCP [22]. The observed Debye rings were in good agreement with both the calculated profiles of HA (hex) and HA (mono) in terms of intensity and positions (see Fig. 6). As confirmed in the contrast-tuned

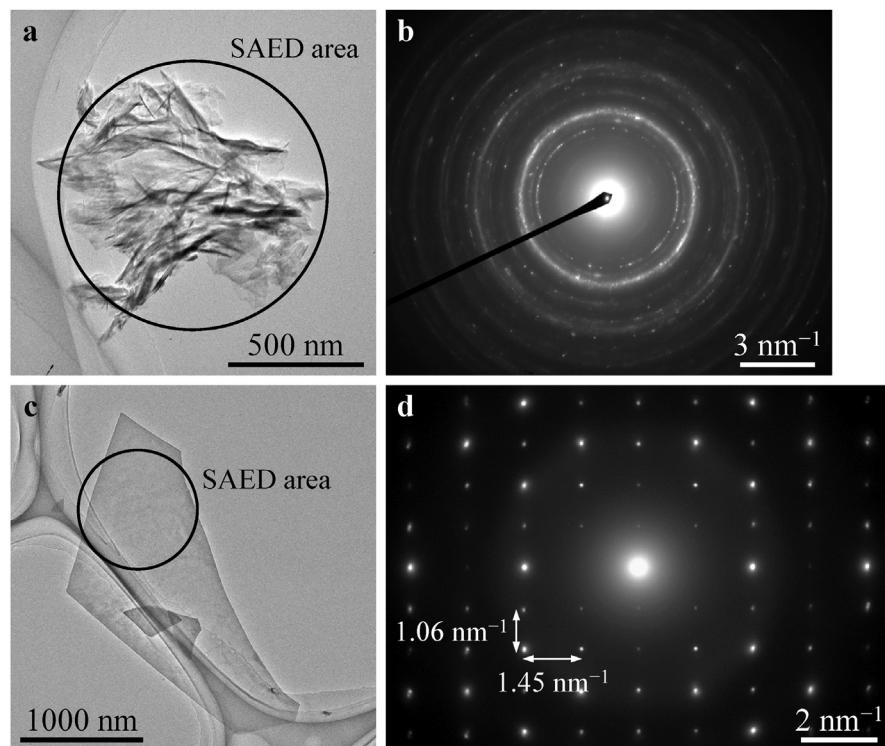


**Fig. 5.** TEM images (a, c) and the corresponding SAED patterns (b, d) of the fragments sampled from the coating layer on the LAB-processed BA3 substrate. The SAED patterns (b) and (d) were measured from the circled area of the fragments in (a) and (c), respectively.

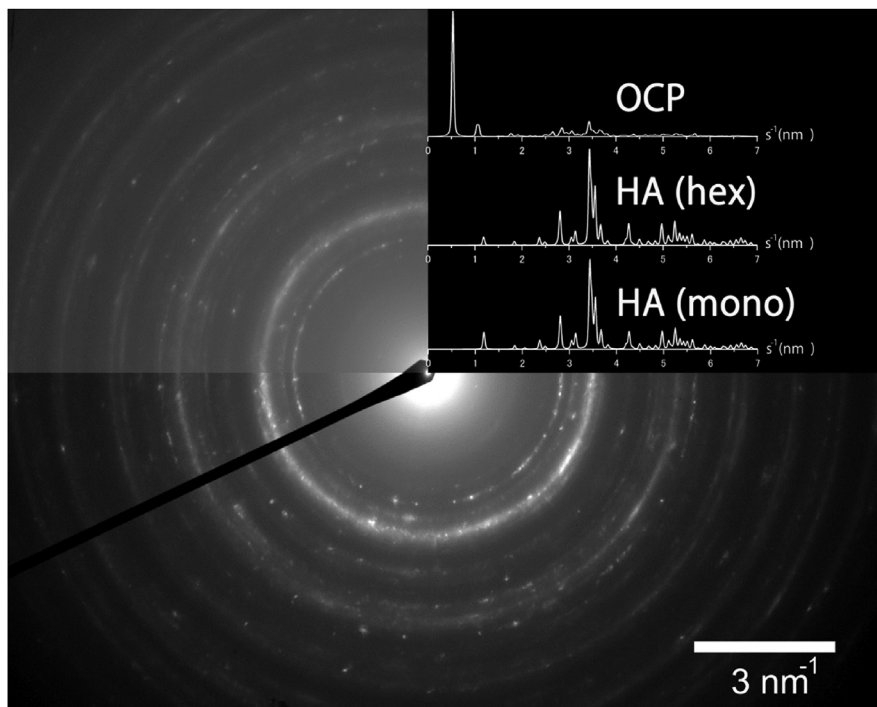


**Fig. 6.** SAED pattern of the aggregated fragments [Fig. 5 (a)] sampled from the coating layer on the BA3 substrate after the LAB process, in comparison with the calculated diffraction profiles (upper right) of HA (hex), HA (mono), and OCP. The upper left region of the SAED pattern was used to tweak the image contrast for comparison with the calculated OCP profile (at  $s = 0.5 \text{ nm}^{-1}$ ).

SAED pattern (upper left region in Fig. 6), no ring was observed at  $s = 0.5 \text{ nm}^{-1}$  ascribed to the 100 strongest reflections of OCP, indicating the presence of little or no OCP phase. These results suggest that the aggregated fragments in Fig. 5 (a) are composed of HA (hex), HA (mono), or their mixtures, but do not involve OCP.

The plate-like single fragment [Fig. 5 (c)] obtained from the same coating layer gave a spotty SAED pattern [Fig. 5 (d)], suggesting a single crystalline nature. The whole pattern exhibited 2 mm symmetry, and the horizontal and vertical spot-to-spot distances were  $1.45$  and  $1.06 \text{ nm}^{-1}$ , respectively. This experimental SAED pattern was compared with the calculated patterns for three different CaP crystalline phases: HA (hex), HA (mono), and OCP (Fig. 7) [22]. The calculated pattern of HA (hex) along the [210] zone axis [Fig. 7 (b)] does not produce a series of spots with the vertical distance of  $1.06 \text{ nm}^{-1}$ , which was apparent in the measured pattern [see Fig. 7 (a)], indicating that the observed pattern is lower in crystallographic symmetry than the hexagonal one. The lower symmetry HA (mono) model along the [110] zone axis [Fig. 7 (c)] shows a well matched pattern with the measured one with respect to the pattern symmetry along with the spot-to-spot distances although some spots are lower in intensity or absent (indicated by dotted squares). The OCP model along the [110] zone axis [Fig. 7 (d)] also shows a similar pattern to the measured one

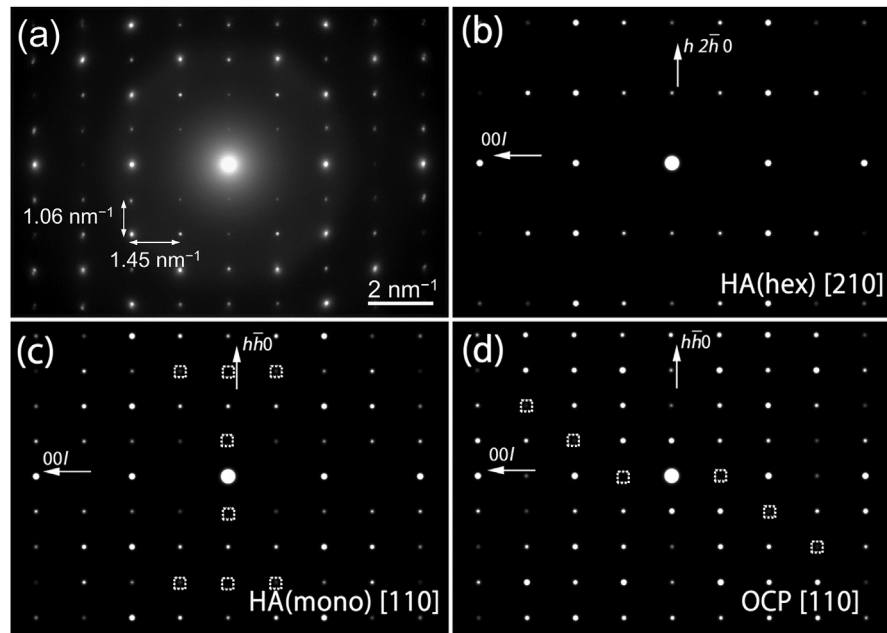


**Fig. 7.** The measured SAED pattern [(a): same as Fig. 5 (d)] from the circled area of the plate-like single fragment in Fig. 5 (c), which was sampled from the coating layer on the LAB-processed BA3 substrate. The calculated diffraction patterns of HA (hex) along the [210] zone axis (b), HA (mono) along the [110] zone axis (c), and OCP along the [110] zone axis (d).

but exhibits a lower pattern symmetry due to the lack or weakening of certain spots (indicated by dotted squares). Although all of the three candidates did not fully match with the measured SAED pattern, one can judge that HA (mono) is the most appropriate structure for the plate-like single fragment. The slight discrepancy in spot intensity between the measured [Fig. 7 (a)] and calculated [Fig. 7 (c)] SAED patterns might be due to the radiation damage [22].

According to the analytical results described above, the CaP layer formed on the LAB-processed BA3 resin surface is considered to contain HA as the main crystal-line phase. Coexistence of a trace amount of OCP and/or an amorphous phase is not denied, although they were not detected under the tested analytical conditions. Similar TEM results were obtained also for the CaP fragments sampled from the LAB-processed BCV resin (Fig. 8).

### 3.3. SBF test for preliminary osteoconductivity assessment

The SBF test confirmed the HA-forming ability of the LAB-processed CaP-coated resin surfaces. As shown in Figs. 9 and 10 (d, f), a dense HA layer formed on the surfaces of the LAB-processed BA3 and BCV substrates after immersion in SBF for 3 days. The initial CaP (HA) layers on the LAB-processed BA3 and BCV resins were extremely thin and undetectable using thin-film XRD [Figs. 9 and 10 (e)]; however, they grew and thickened in SBF, providing clear diffraction

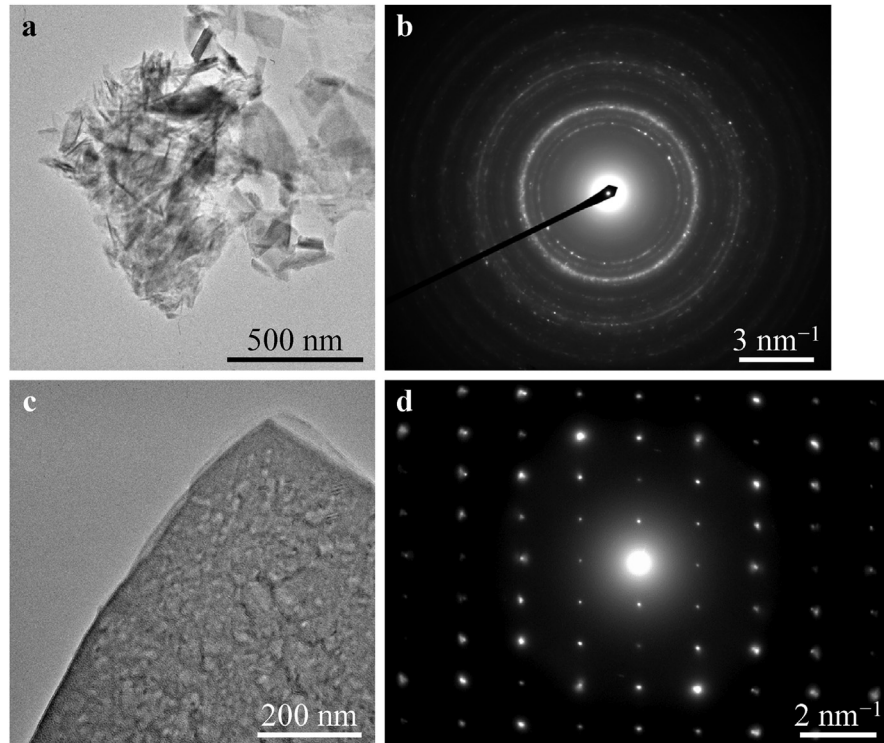


**Fig. 8.** TEM images (a, c) and the corresponding SAED patterns (b, d) of the fragments sampled from the coating layer on the LAB-processed BCV substrate. The SAED patterns (b) and (d) were measured from the fragments in (a) and (c), respectively.

peaks characteristic to HA [(002) and (211) at  $2\theta$  of approximately 26 and 32°, respectively] after 3 days [Figs. 9 and 10 (f)]. The untreated substrates revealed no apparent changes on their surfaces after the same SBF test [Figs. 9 and 10 (a, c)]. These results prove that the untreated resin surfaces lack HA-forming ability in SBF. In general, materials that possess HA-forming ability in SBF exhibit osteoconductivity; they induce bonelike HA formation in the body environment as well

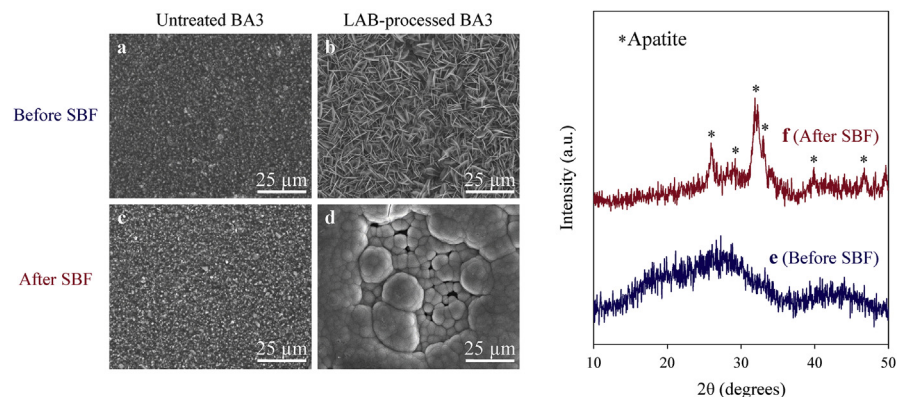


**Fig. 9.** SEM images (a–d) and thin-film XRD profiles (e, f) of the surfaces of the untreated (a, c) and LAB-processed (b, d) BA3 substrate, before (a, b, e) and after (c, d, f) the SBF test.

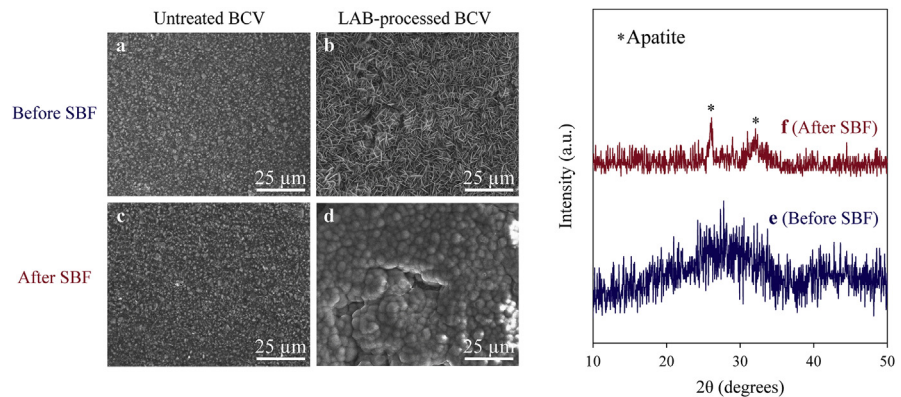


**Fig. 10.** SEM images (a–d) and thin-film XRD profiles (e, f) of the surfaces of the untreated (a, c) and LAB-processed (b, d) BCV substrate, before (a, b, e) and after (c, d, f) the SBF test.

and integrate with human hard tissues through the interfacial HA layer [18]. Thus, the results indicate improved osteoconductivity of the LAB-processed resin surfaces compared to the untreated surfaces.

### 3.4. Advantages and potential of the LAB process

The obtained results demonstrated the potential use of the LAB process for surface functionalization of the light-cured dental composite resins in endodontic treatments. As presented in Figs. 1 and 3, the LAB process produced a CaP layer on the resins, although the coating coverage still needs to be improved. CaP-coated implants have been reported to indicate improved osteoconductivity compared to the uncoated implants *in vivo* [23]. Therefore, the CaP-coated resin surface would be expected to exhibit better osteoconductivity than the untreated surface. This hypothesis was verified using the SBF test, in which the LAB-processed CaP-coated resin surfaces revealed HA-forming ability in SBF, whereas the untreated surfaces did not (Figs. 9 and 10). These results demonstrate that the LAB-processed resin has a cementum-like osteoconductive surface in part, similar to the natural tooth root surface. With such an artificially created cementum-like surface portion, the LAB-processed resin is expected to integrate better with the surrounding alveolar bone compared with the untreated resin. Furthermore, with appropriate occlusal loads, it may promote reconstruction of the periodontal attachment through the regeneration of periodontal ligament-like tissue [24], although this should be verified in future *in vivo* studies. Effects of the LAB process on the mechanical and chemical properties of resins should also be clarified in future studies.

The LAB process is a rapid (30 min) single-step process that can be carried out under normal pressure and temperature in a neutral aqueous solution containing biomineral ions. Unlike other conventional HA coating techniques, the LAB process enables area-specific coating, that is, only a target region (laser-irradiated region) on a

substrate surface is coated and functionalized by the LAB process [12, 13, 14, 15, 16]. Biological properties of the CaP layer might be further improved and tailored by immobilizing therapeutic components into the layer. Note that it is possible to immobilize therapeutic agents such as zinc (trace element with antibacterial activity along with potential therapeutic effects in hard tissue regeneration [25]) into CaP layers using the LAB process [15]. The thus-functionalized resin surfaces would exhibit osteoconductivity along with additional therapeutic effects depending on the component immobilized in the CaP layer. With such an approach using the LAB process, endodontic treatments using composite resins would evolve further and become more effective and reliable.

#### 4. Conclusion

The LAB process was effective in the CaP coating on the light-cured dental composite resins, although the coating coverage needs to be improved further. The coating layer contained HA as a main crystalline phase and the coating coverage depended on the laser wavelength and the type of resin used. The SBF test suggested that the LAB-processed CaP-coated resin surfaces exhibit osteoconductivity. The LAB process described herein can be a potential new tool for the creation of a cementum-like osteoconductive surface on dental composite resins that may lead to better integration with the surrounding alveolar bone and evolution of endodontic treatments using composite resins.

#### Declarations

##### Author contribution statement

A. Joseph Nathanael: Performed the experiments; Analyzed and interpreted the data; Wrote the paper.

Ayako Oyane: Conceived and designed the experiments; Analyzed and interpreted the data; Contributed reagents, materials, analysis tools or data; Wrote the paper.

Maki Nakamura: Performed the experiments; Analyzed and interpreted the data.

Kenji Koga: Performed the experiments; Analyzed and interpreted the data; Contributed reagents, materials, analysis tools or data.

Erika Nishida: Performed the experiments; Contributed reagents, materials, analysis tools or data.

Saori Tanaka: Conceived and designed the experiments; Contributed reagents, materials, analysis tools or data.

Hirofumi Miyaji: Conceived and designed the experiments; Wrote the paper.

## Funding statement

This work was supported by JSPS KAKENHI (JP15F15331, JP17H02093, JP16K11822, and JP16K11538).

## Competing interest statement

The authors declare no conflict of interest.

## Additional information

No additional information is available for this paper.

## Acknowledgements

We thank Ms. Ikuko Sakamaki from AIST for technical support.

## References

- [1] J.L. Ferracane, Resin composite—state of the art, *Dent. Mater.* 27 (2011) 29–38.
- [2] A.P.P. Fugolin, C.S. Pfeifer, New resins for dental composites, *J. Dent. Res.* 96 (2017) 1085–1091.
- [3] K.D. Jandt, B.W. Sigusch, Future perspectives of resin-based dental materials, *Dent. Mater.* 25 (2009) 1001–1006.
- [4] J. Rud, E.C. Munksgaard, J.O. Andreason, V. Rud, E. Asmussen, Retrograde root filling with composite and a dentin-bonding agent. 1, *Endont. Dent. Traumatol.* 7 (1991) 118–125.
- [5] M. Trope, C. Lost, H.J. Schmitz, S. Friedman, Healing of apical periodontitis in dogs after apicoectomy and retrofilling with various filling materials, *Oral Surg. Oral Med. Oral Pathol. Oral Radiol. Endod.* 81 (1996) 221–228.
- [6] W. Suchanek, M. Yoshimura, Processing and properties of hydroxyapatite-based biomaterials for use as hard tissue replacement implants, *J. Mater. Res.* 13 (1998) 94–117.
- [7] S.V. Dorozhkin, Calcium orthophosphate bioceramics, *Ceram. Intern.* 41 (2015) 13913–13966.
- [8] N. Eliaz, N. Metoki, Calcium phosphate bioceramics: a review of their history, structure, properties, coating technologies and biomedical applications, *Materials* 10 (2017) 334.

- [9] S.R. Paital, N.B. Dahotre, Calcium phosphate coatings for bio-implant applications: materials, performance factors, and methodologies, *Mater. Sci. Eng. R* 66 (2009) 1–70.
- [10] L. Sun, C.C. Berndt, K.A. Gross, A. Kucuk, Material fundamentals and clinical performance of plasma-sprayed hydroxyapatite coatings: a review, *J. Biomed. Mater. Res. Appl. Biomater.* 58 (2001) 570–592.
- [11] M. Nakamura, A. Oyane, Physicochemical fabrication of calcium phosphate-based thin layers and nanospheres using laser processing in solutions, *J. Mater. Chem. B* 4 (2016) 6289–6301.
- [12] A. Oyane, I. Sakamaki, Y. Shimizu, K. Kawaguchi, N. Koshizaki, Liquid-phase laser process for simple and area-specific calcium phosphate coating, *J. Biomed. Mater. Res. A* 100A (2012) 2573–2580.
- [13] A. Oyane, I. Sakamaki, A. Pyatenko, M. Nakamura, Y. Ishikawa, Y. Shimizu, K. Kawaguchi, N. Koshizaki, Laser-assisted calcium phosphate deposition on polymer substrates in supersaturated solutions, *RSC Adv.* 4 (2014) 53645–53648.
- [14] A. Oyane, I. Sakamaki, Y. Shimizu, K. Kawaguchi, Y. Sogo, A. Ito, N. Koshizaki, Laser-assisted biomimetic process for calcium phosphate coating on a hydroxyapatite ceramic, *Key Eng. Mater.* 529–530 (2013) 217–222.
- [15] A. Oyane, N. Matsuoka, K. Koga, Y. Shimizu, M. Nakamura, K. Kawaguchi, N. Koshizaki, Y. Sogo, A. Ito, H. Unuma, Laser-assisted biomimetic process for surface functionalization of titanium metal, *Col. Interf. Sci. Commun.* 4 (2015) 5–9.
- [16] M. Mahanti, M. Nakamura, A. Pyatenko, I. Sakamaki, K. Koga, A. Oyane, The mechanism underlying calcium phosphate precipitation on titanium via ultraviolet, visible, and near infrared laser-assisted biomimetic process, *J. Phys. D Appl. Phys.* 49 (10 pp) (2016) 304003.
- [17] M. Uchida, A. Oyane, H.M. Kim, T. Kokubo, A. Ito, Biomimetic coating of laminin–apatite composite on titanium metal and its excellent cell-adhesive properties, *Adv. Mater.* 16 (2004) 1071–1074.
- [18] T. Kokubo, H. Takadama, How useful is SBF in predicting in vivo bone bioactivity? *Biomaterials* 27 (2006) 2907–2915.
- [19] K. Onuma, A. Ito, Cluster growth model for hydroxyapatite, *Chem. Mater.* 10 (1998) 3346–3351.
- [20] A. Oyane, K. Onuma, T. Kokubo, A. Ito, Clustering of calcium phosphate in the system  $\text{CaCl}_2\text{--H}_3\text{PO}_4\text{--KCl--H}_2\text{O}$ , *J. Phys. Chem. B* 103 (1999) 8230–8235.



- [21] A. Dey, P.H.H. Bomans, F.A. Müller, J. Will, P.M. Frederik, G. de With, N.A.J.M. Sommerdijk, The role of prenucleation clusters in surface-induced calcium phosphate crystallization, *Nat. Mater.* 9 (2010) 1010–1014.
- [22] M. Espanol, J. Portillo, J.M. Manero, M.P. Ginebra, Investigation of the hydroxyapatite obtained as hydrolysis product of  $\alpha$ -tricalcium phosphate by transmission electron microscopy, *CrystEngComm* 12 (2010) 3318–3326.
- [23] R.A. Surmenev, M.A. Surmeneva, A.A. Ivanova, Significance of calcium phosphate coatings for the enhancement of new bone osteogenesis – a review, *Acta Biomater.* 10 (2014) 557–579.
- [24] T. Kano, R. Yamamoto, A. Miyashita, K. Komatsu, T. Hayakawa, M. Sato, S. Oida, Regeneration of periodontal ligament for apatite-coated tooth-shaped titanium implants with and without occlusion using rat molar model, *J. Hard Tissue Biol.* 21 (2012) 189–202.
- [25] A. Ito, H. Kawamura, M. Otsuka, M. Ikeuchi, H. Ohgushi, K. Ishikawa, K. Onuma, N. Kanzaki, Y. Sogo, N. Ichinose, Zinc-releasing calcium phosphate for stimulating bone formation, *Mater. Sci. Eng. C* 22 (2002) 21–25.